Proc. Natl. Acad. Sci. USA
Vol. 95, pp. 3661–3666, March 1998
Cell Biology

Structural changes at microtubule ends accompanying GTP hydrolysis: Information from a slowly hydrolyzable analogue of GTP, guanylyl (α,β)methylenediphosphonate

THOMAS MÜLLER-REICHERT*, DENIS CHRÉTIEN, FEDOR SEVERIN, AND ANTHONY A. HYMAN

Cell Biology Program, European Molecular Biology Laboratory, Meyerhofstrasse 1, Postfach 1022.09, D-69117, Heidelberg, Germany

Communicated by Kai Simons, European Molecular Biology Laboratory, Heidelberg, Germany, December 29, 1997 (received for review December 12, 1997)

ABSTRACT **Microtubules are dynamic polymers that interconvert between periods of slow growth and fast shrinkage. The energy driving this nonequilibrium behavior comes from the hydrolysis of GTP, which is required to destabilize the microtubule lattice. To understand the mechanism of this destabilization, cryo-electron microscopy was used to compare the structure of the ends of shrinking microtubules assembled in the presence of either GTP or the slowly hydrolyzable analogue guanylyl (α,β)methylenediphosphonate (GMPCPP). Depolymerization was induced by cold or addition of calcium. With either nucleotide, we have observed curled oligomers at the ends of shrinking microtubules. However, GDP oligomers were consistently more curved than GMPCPP oligomers. This difference in curvature between depolymerizing GDP and GMPCPP protofilaments suggests that GTP hydrolysis is accompanied by an increase in curvature of the protofilaments, thereby destabilizing the lateral interactions between tubulin subunits in the microtubule lattice.**

Microtubules are polar macromolecules composed of tubulin α-β heterodimers (1). The head-to-tail alignment of these tubulin dimers forms protofilaments, which are juxtaposed to form the cylindrical microtubule wall (2). Microtubules show alternating phases of growth and shrinkage. The interconversion between these phases is unpredictable, a process known as dynamic instability (3–7). GTP hydrolysis is thought to play a key role in regulating this dynamic behavior of microtubule growth and shrinkage. GTP bound to β-tubulin is hydrolyzed to GDP during—or soon after—microtubule assembly (8–10). The resulting GDP microtubule lattice is unstable. In contrast, work with nonhydrolyzable analogues of GTP has shown that a GTP-like lattice is stable (11, 12).

How does GTP hydrolysis destabilize the microtubule lattice? There is some evidence that tubulin can take up different conformational states according to its nucleotide state. The GTP- and GDP-bound states of tubulin in the dimeric form differ by Raman spectroscopy (13) in α-helix and anti-parallel β-sheet content. Analysis of tubulin structure by cryo-electron microscopy (EM) has shown that in the presence of a nonhydrolyzable analogue of GTP, guanylyl (α,β)methylenediphosphonate (GMPCPP), the average length of the tubulin dimer is 0.3 nm longer than in microtubules consisting of GDP-tubulin (14). These data combine to suggest that GTP hydrolysis changes the conformation of the tubulin dimer.

How could structural changes in the tubulin dimer induced by GTP hydrolysis destabilize the microtubule lattice? It has been known for a long time that the structure of microtubule ends is different between growing and shrinking phases. Microtubules grow by elongation of tubulin sheets that later close to form the cylindrical wall (15–17), whereas microtubules depolymerize by coiling of individual protofilaments and end-wise release of curled oligomers (18–20) with a radius of curvature of about 18–20 nm (19). Combined with the data discussed above, suggesting that tubulin could take up two conformations, the striking images of curled oligomers during depolymerization suggested the following model: when liganded with GTP, tubulin is in a "straight" conformation. Upon GTP hydrolysis, the tubulin molecule would tend to adopt a "curved" conformation (21). This model was developed by Mandelkow *et al*. (19) to suggest that GTP hydrolysis, by increasing the curvature of the protofilaments, forces them to peel off the microtubule wall and that this change in curvature is the driving force for microtubule depolymerization. These models suggest that the GTP protofilament should be less curved than GDP protofilaments. However, individual GTP protofilaments have never been observed by electron microscopy.

Here, we have looked at the curvature of protofilaments liganded with GMPCPP, a nonhydrolyzable analogue of GTP, to trap protofilaments in the GTP state (12, 14). We have compared this curvature with that of protofilaments liganded with GDP. We show that both GDP and GMPCPP protofilaments are curved during microtubule disassembly. However, GDP protofilaments are more curved than GMPCPP protofilaments. This result suggests a difference in structure between GTP and GDP protofialments and is compatible with the model suggesting that an increase in curvature could drive microtubule depolymerization.

MATERIALS AND METHODS

Tubulin Preparation and GMPCPP Synthesis. Calf brain tubulin was purified by two cycles of assembly/disassembly in the presence of glycerol and subsequent phosphocellulose chromatography as described previously (22). Tubulin concentration was determined from video-microscope measurements using an association constant of 3.8 $\mu M^{-1} \cdot s^{-1}$, thus measuring the concentration of active tubulin (23). Axonemes were isolated from *Tetrahymena thermophila* (24). GMPCPP was synthesized as described (12), except that the final product was purified by two rounds of precipitation in ethanol. Tubulin assembly was performed at 37°C in BRB80 (80 mM Pipes/1 mM EGTA/1 mM $MgCl_2$, pH 6.8 with KOH) + 1 mM GTP or 0.1 mM GMPCPP.

Cryo-EM. The ends of shrinking microtubules were analyzed on self-assembled microtubules according to the methods of Chrétien *et al.* (17). For observation of cold-

The publication costs of this article were defrayed in part by page charge payment. This article must therefore be hereby marked "*advertisement*" in accordance with 18 U.S.C. §1734 solely to indicate this fact.

Abbreviations: EM, electron microscopy; DIC, differential interference contrast; GMPCPP, guanylyl (α,β)methylene]diphosphonate.

*To whom reprint requests should be addressed. e-mail: reichert@embl-heidelberg.de.

depolymerized GDP microtubules, tubulin concentration was adjusted to 9 mg/ml, and the microtubules were assembled for 3.5 min at 37°C. A 4-μl sample was then transferred to the holey carbon-coated grid, and depolymerization was initiated by lowering the temperature of the sample to about 4°C using a cold stream of air blown onto the specimen. We checked the extent of evaporation by measuring the conductivity of a 1 M NaCl solution under these conditions. Evaporation was limited to 15% over the 30 sec needed to cool the specimen. GMPCPP microtubules were assembled at a tubulin concentration of 0.4 mg/ml for 30 min and subsequently depolymerized for 1 min on ice to ensure that all microtubules were in the shrinking phase. Using the same tubulin concentration for GMPCPP as was used for GTP resulted in an extensive end to end annealing of the microtubules that render the analysis of the ends impossible. For calcium-induced depolymerization, GDP microtubules were assembled at either 5 mg/ml or 9 mg/ml tubulin concentration for various times, and GMPCPP microtubules were polymerized for 1 h at a tubulin concentration of 0.4 mg/ml. Depolymerization was started by mixing rapidly 9 volumes of microtubule solution with 1 volume of a 10× stock of $CaCl_2$ to give a final concentration of either 4 or 40 mM. The sample was then rapidly transferred to a prewarmed carbon-coated grid and prepared for cryo-EM. Storage and observation of the samples were performed as described previously (17). The structure of microtubule ends and of depolymerization products was analyzed on enlarged prints. Radii of curvature were determined by overlaying circles of defined curvature on the prints.

Site Occupancy of GMPCPP Microtubules. Microtubules were polymerized from 300 μl of 5 mg/ml tubulin preincubated with GMPCPP on ice for 15 min (GMPCPP tubulin) for 30 min at 37°C. The nucleotides were extracted as described (25) and analyzed on a monoQ 1.6/5 column using a SMART system (Pharmacia). The column was equilibrated with BRB80, and the sample was loaded and eluted with 20 column volumes of gradient 0–400 mM NaCl in BRB80. GTP, GDP, and GMPCPP separated well. Because GMPCPP tubulin is free of GTP, the tubulin concentration was calculated using the N-site GTP. The site occupancy of GMPCPP was calculated by comparing GMPCPP with GDP. GMPCPP site occupancy was 70%. To increase the site occupancy to 90%, tubulin was equilibrated with GMPCPP using a desalting column HR 10/10 (Pharmacia). The column was preequilibrated with 10 ml of 100 μM GMPCPP in BRB80. Two hundred microliters of cycled tubulin (15 mg/ml) in 100 μM GMPCPP in BRB80 was loaded. Protofilament curvature during depolymerization was examined at high site occupancy. No difference in curvature of the protofilaments was noticed when microtubules depolymerize (data not shown).

Video-Enhanced Differential Interference Contrast (DIC) Light Microscopy. Video-DIC light microscopy was performed as described previously (17) to analyze the depolymerization rates of axoneme-seeded microtubules. Measurements included both plus- and minus-ended microtubules. We have used special homemade metal chambers to induce cold depolymerization of the microtubules. Long microtubules

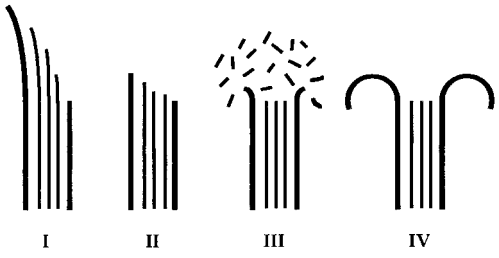

FIG. 1. Classification of microtubule ends as observed by cryo-EM. Four classes of ends were defined: I, curved sheets; II, tapered or blunt ends; III, tapered or blunt ends surrounded by a "cloud" of oligomeric structures; and IV, ends showing curved oligomers.

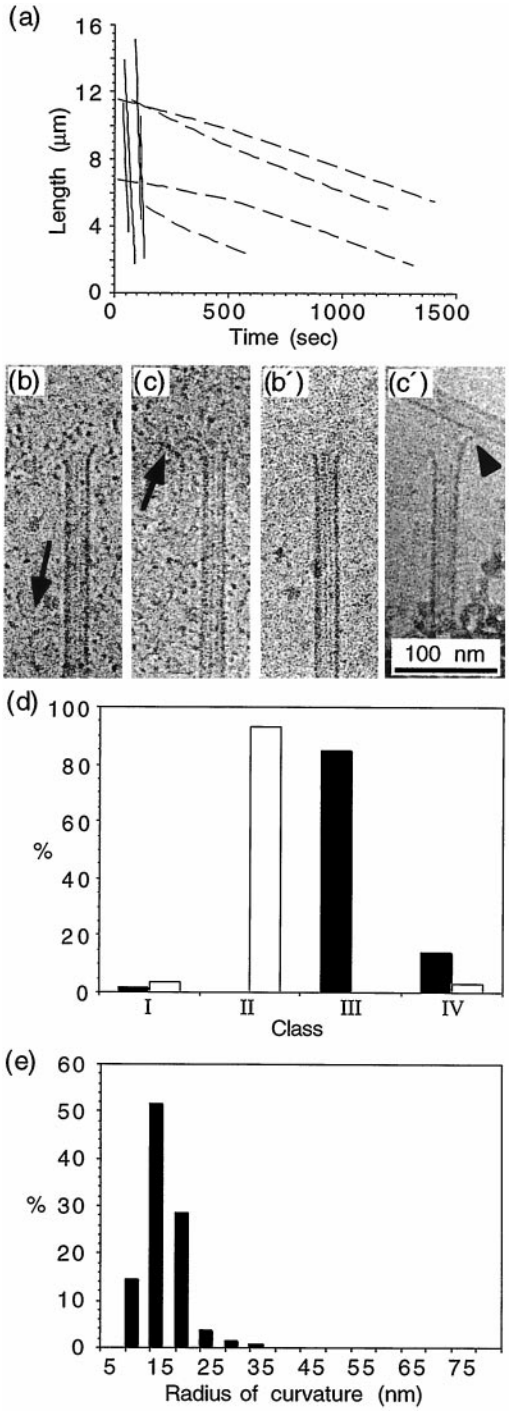

FIG. 2. Cold-induced depolymerization of GDP and GMPCPP microtubules. (*a*) Length versus time plots of GDP (plain lines) and GMPCPP microtubules (dotted lines) obtained by video-DIC light microscopy. Depolymerization rates of -20.3 ± 4.9 μm/min and -0.3 ± 0.1 μm/min were measured for GDP and GMPCPP microtubules, respectively. (*b*, *c*) Ends of depolymerizing GDP microtubules. Curved oligomeric structures are indicated by arrows. (*b′*, *c′*) Ends of depolymerizing GMPCPP microtubules as observed by cryo-electron microscopy. The arrowhead in (*c′*) shows a curled end. (*d*) Percentage of end types observed after cold depolymerization of GDP (black bars) and GMPCPP microtubules (open bars). About 85% of the GDP microtubule ends showed oligomeric structures, and 95% of the GMPCPP microtubules showed tapered or blunt ends. (*e*) Curvature of the oligomers observed during cold depolymerization of GDP microtubules. The average radius of curvature was 19 ± 4.1 nm.

were allowed to grow at 37°C by placing the specimen chambers on a thermostated plate. To induce microtubule depolymerization, the specimen chambers were mounted on the stage of the light microscope, and metal blocks were placed on top of the specimen chambers. The metal blocks and both the objective and the condenser of the light microscope were cooled by a solution containing ~80% water and ~20% methanol using a brass collar and cooling tubes. The temperature inside the specimen chamber could be accurately controlled using a fine thermocouple. The lowest temperature achieved was 7°C. The temperature could be reduced from 37°C to 7°C in about 3–4 min. The conditions used for assembly were as described for the cryo-EM experiments, except that the tubulin concentrations were 1.8 and 0.25 mg/ml for assembly in the presence of GTP and GMPCPP, respectively. To examine calcium-induced disassembly of microtubules, we used glass chambers made of a glass slide and a coverslip (5). The microtubules were allowed to grow at 37°C as before, and the specimen chamber was placed on the stage of the microscope. The stage, the objective, and the condenser were heated using a homemade device to ensure a temperature of 37°C inside the specimen chamber. Depolymerization was induced by perfusing a large volume of prewarmed tubulin at the same concentration (and in the same buffer as was used for assembly) and containing either 4 or 40 mM calcium. The tubulin concentration was 2 mg/ml and 0.1 mg/ml for assembly in the presence of GTP and GMPCPP, respectively. Analysis of the video sequences and rate measurements was performed as described (17).

RESULTS

We wanted to examine the structure of GMPCPP microtubules to investigate whether the curvature of protofilaments during disassembly was changed by GTP hydrolysis. Study of the depolymerization products of GMPCPP microtubules is hampered by the fact that under normal conditions of isothermal dilution, GMPCPP microtubules do not depolymerize. We destabilized GMPCPP microtubules using either cold depolymerization or calcium (12). To confirm that GMPCPP microtubules depolymerize in the presence of cold or calcium without hydrolysis, we labeled the γ phosphate of GMPCPP

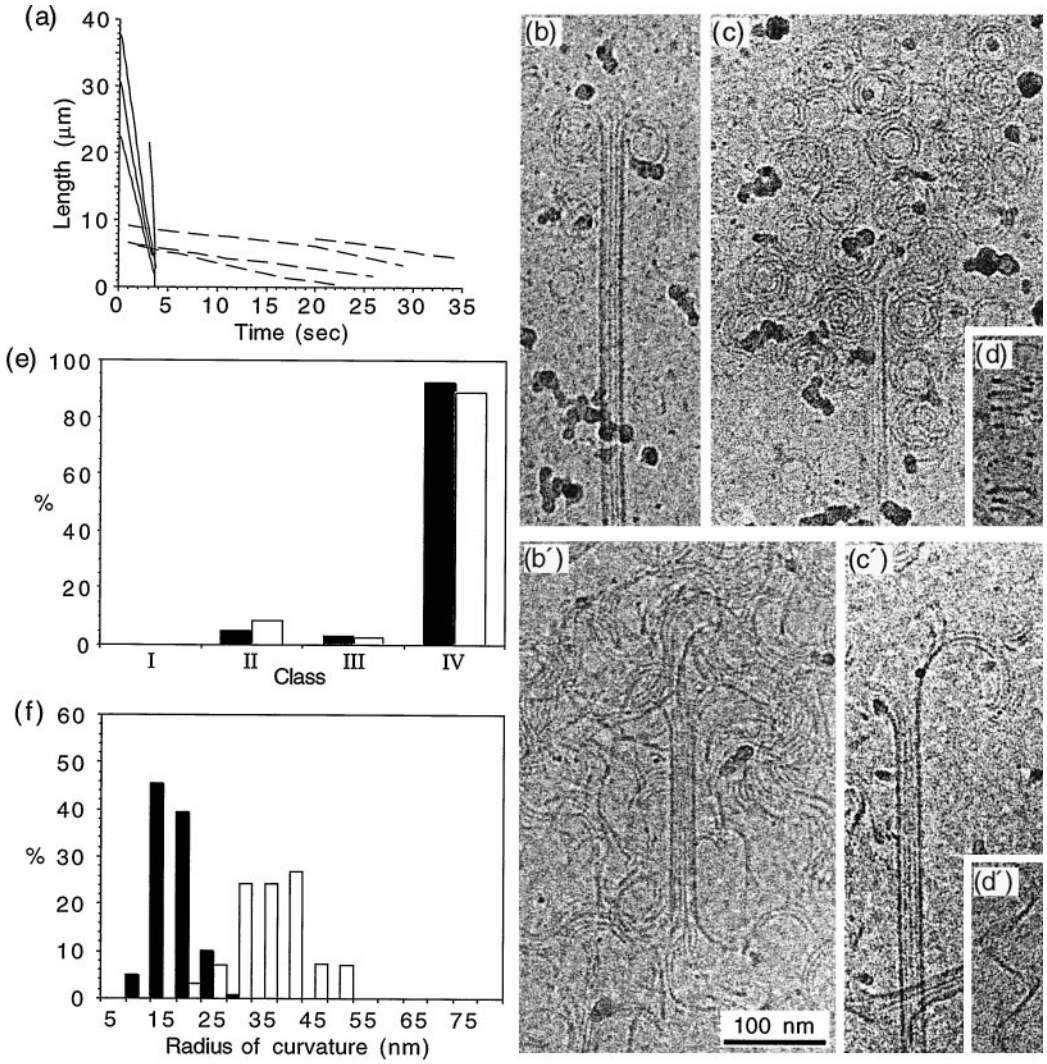

FIG. 3. Depolymerization of GDP and GMPCPP microtubules in the presence of 4 mM calcium. (*a*) Length versus time plots of GDP (plain lines) and GMPCPP microtubules (dotted lines). Depolymerization rates of −611 ± 125 μm/min and −13.0 ± 3.2 μm/min were measured for GDP and GMPCPP microtubules, respectively. (*b–d*) Depolymerization products of GDP microtubules. (*b′–d′*) Depolymerization products of GMPCPP microtubules. Curved oligomeric structures (*b*, *b′*, *c*, *c′*) and spirals of protofilaments (*d*, *d′*) were observed in both cases. (*e*) Percentage of end types observed after calcium depolymerization of GDP (black bars) and GMPCPP microtubules (open bars). About 90% of both GDP and GMPCPP microtubule ends displayed curved oligomers. (*f*) Curvature of the oligomers observed during calcium depolymerization of the GDP (black bars) and GMPCPP microtubules (open bars). The average radius of curvature was 20 ± 4.1 nm and 38.6 ± 7.1 nm for GDP and GMPCPP oligomers, respectively.

with ^{32}P. Trace amounts of [γ-^{32}P]GMPCPP were added during polymerization in the presence of GMPCPP. GMPCPP microtubules were recovered by sedimentation through sucrose, and GMPCPP hydrolysis was monitored by thin layer chromatography (12). Although calcium and cold induced depolymerization of microtubules, neither induced detectable hydrolysis of GMPCPP (data not shown and ref. 12). Because GTP is hydrolyzed in the microtubule lattice to GDP, the structures observed at the depolymerizing ends of GTP microtubules reflect disassembly of a GDP tubulin lattice. Therefore, microtubules assembled in the presence of GTP will be called GDP microtubules. Similarly, microtubules assembled in the presence of GMPCPP will be called GMPCPP microtubules. Microtubules were grown in the presence of either nucleotide and subjected to cold or to calcium. The shrinking rates were measured using video-DIC light microscopy, and the depolymerization products were analyzed using cryo-EM. To better quantify the effects of GTP hydrolysis on microtubule ends, four classes were defined (Fig. 1): I, ends showing outwardly curved sheets; II, blunt or slightly tapered ends; III, blunt or slightly tapered ends surrounded by a cloud of oligomeric structures; and IV, ends showing curved oligomeric structures. Although class I is characteristic of growing microtubules and class III and class IV are characteristic of shrinking microtubules, class II can be seen in either growing or shrinking microtubules.

Cold-Induced Depolymerization. The destabilization of microtubules by cold was characterized initially using video-DIC light microscopy. Microtubules were nucleated from axonemes in the presence of either nucleotide and cooled to 7°C on the stage of the light microscope. Length versus time plots of cold-depolymerizing GDP and GMPCPP microtubules are given in Fig. 2*a*. GDP microtubules were found to shrink at a rate of -20.3 ± 4.9 μm/min, whereas GMPCPP microtubules depolymerized very slowly at a rate of -0.3 ± 0.1 μm/min. To characterize the structure of the ends by cryo-EM, microtubules were self-assembled in a test tube. Samples of microtubules assembled in the presence of GTP were transferred to the EM grid and subjected to a cold stream of air to lower the temperature to ~4°C before vitrification. Cold-depolymerizing GDP microtubules observed by cryo-EM showed 85% of microtubules surrounded by a "cloud" of depolymerization products (Fig. 2 *b* and *d*) or short and curved oligomers (Fig. 2 *c* and *d*). Oligomeric structures were also observed in the background (Fig. 2 *b* and *c*, arrows). The average radius of curvature of the curved GDP oligomers was 19.0 ± 4.1 nm (Fig. 2*e*).

GMPCPP microtubules were incubated for 1 min on ice before cryo-EM preparation due to the very low rate of shrinkage. A total of 95% of the cold-depolymerized GMPCPP microtubules were identified with tapered or blunt ends (class II) (Fig. 2 *b′* and *d*) and showed occasionally short and curved extensions (Fig. 2*c′*, arrowhead); the remaining microtubules showed very short and curved extensions (class IV). Very few products of depolymerization could be identified in the background. The curved structures observed at the ends of GMPCPP microtubules were too short to be measured accurately.

Calcium-Induced Depolymerization. Because the rate of depolymerization of GMPCPP microtubules induced by cooling was too slow to identify a significant number of depolymerization products, we decided to induce depolymerization using calcium. To measure the depolymerization rates, long microtubules were grown from axonemes, and the specimen chambers were perfused with a prewarmed tubulin solution containing 4 mM calcium. Fig. 3*a* compares the length versus time plots of microtubules depolymerized in the presence of 4 mM calcium (note the difference in time scale with Fig. 3*a*). GDP microtubules depolymerized at -611 ± 1.25 μm/min compared with -13.0 ± 3.2 μm/min for GMPCPP microtubules. Cryo-EM showed that both the GDP and GMPCPP microtubules depolymerized by release of curved oligomers comprising ring-like structures (Fig. 3 *b*, *b′*, *c*, and *c′*) and spirals of protofilaments (Fig. 3 *d* and *d′*). Roughly 90% of both GDP and GMPCPP microtubules could be identified with curved oligomers at their ends (Fig. 3*e*). The main difference between GDP and GMPCPP oligomers was found in their radii

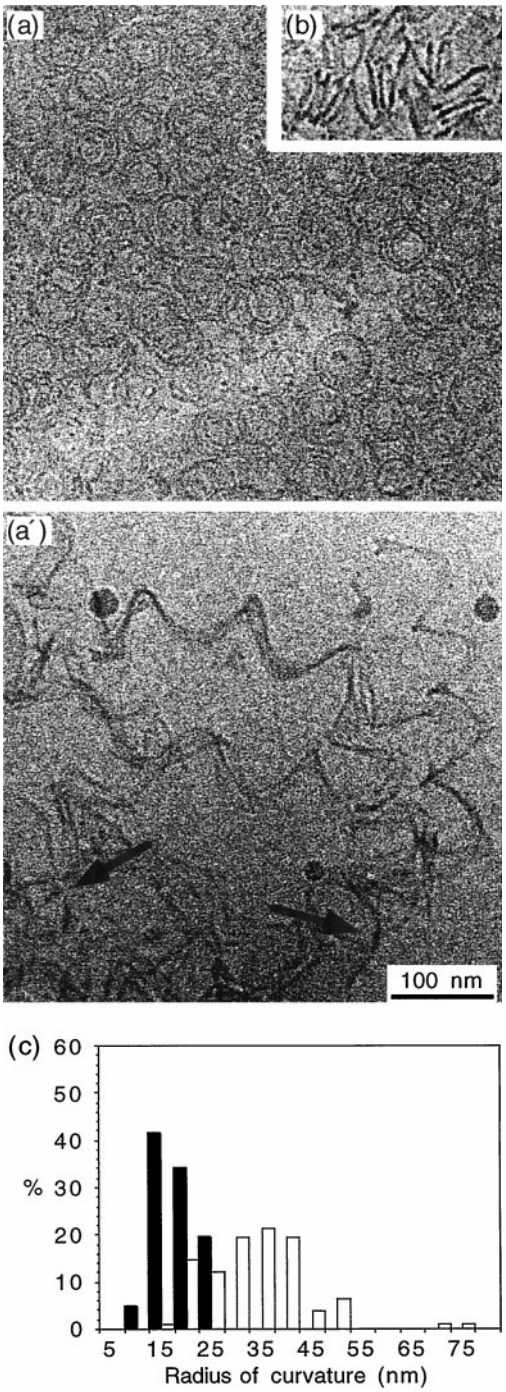

FIG. 4. Depolymerization of GDP and GMPCPP microtubules in the presence of 40 mM calcium. (*a*, *b*) Depolymerization products of GDP microtubules. Curved oligomers (*a*) and spirals of protofilaments, seen as a side view (*b*), were observed. (*a′*) Depolymerization products of GMPCPP microtubules. Long spirals of protofilaments as well as curved oligomers (arrows) were observed in the background. (*c*) Curvature of the oligomeric products of GDP (black bars) and GMPCPP microtubules (open bars). The average radius of curvature was 21.2 ± 4.3 nm and 36.2 ± 10.1 nm for the GDP and GMPCPP oligomers, respectively.

Table 1. Rates of depolymerization of GDP and GMPCPP microtubules and radius of curvature of oligomers

	GDP microtubules		GMPCPP microtubules	
Conditions	Rate, μm/min	Radius, nm	Rate, μm/min	Radius, nm
Cooling	-20.3 ± 4.9 (8, 163)	19.0 ± 4.1 (140)	-0.3 ± 0.1 (8, 274)	ND
4 mM Ca^{2+}	-611 ± 125 (7, 90)	20.0 ± 4.1 (163)	-13.0 ± 3.2 (12, 176)	38.6 ± 7.1 (160)
40 mM Ca^{2+}	ND	21.1 ± 4.3 (123)	-72.0 ± 45.0 (3, 60)	36.2 ± 10.1 (108)

The rates of depolymerization were measured on individual microtubules using video-DIC light microscopy. The two numbers in parentheses indicate the number of microtubules analyzed and the number of rate measurements performed. The radii of curvature were measured on oligomers present at the ends of shrinking microtubules or in the background of the cryo-EM images. The number in parentheses indicates the number of measurements performed. Mean values are given $\pm$ their standard deviation. ND, not determined.

of curvature (Fig. 3*f*). The mean radius of curvature was 20.0 ± 4.1 nm for the GDP oligomers and 38.6 ± 7.1 nm for the GMPCPP oligomers.

Although the shrinking rate of calcium-depolymerized GDP microtubules was 20-fold greater compared with cold-depolymerized GDP microtubules, the radius of curvature of the oligomers remained constant at $\approx$20 nm in both conditions. We asked whether the curvature of the oligomers released from the ends of shrinking GMPCPP microtubules was also independent of calcium concentration. To increase the rate of depolymerization, we increased the calcium concentration to 40 mM. Under these conditions, the rate of depolymerization of GDP microtubules was too fast to be accurately determined. We observed only a cloud of depolymerized oligomers, either coiled oligomers and rings (Fig. 4*a*) or spirals (Fig. 4*b*). The radii of curvature was 21.1 ± 4.3 nm (Fig. 4*c*). Under the same conditions, GMPCPP microtubules depolymerized at -72 ± 45 μm/min. The depolymerization products were mostly long spirals of protofilaments; some curved oligomers could be observed in the background (see arrows in Fig. 4*a′*). We found radii of curvature of 36.2 ± 10.1 nm for the GMPCPP oligomers as seen at 4 mM calcium. Thus, the radius of curvature is independent of calcium concentration, suggesting that we have revealed the intrinsic curvature of the protofilaments. We conclude that protofilaments of GDP microtubules are more curved than those of GMPCPP microtubules.

DISCUSSION

In this paper, we have investigated the mechanisms by which GTP hydrolysis destabilizes microtubules by examining the structure of protofilaments at microtubule ends, with and without nucleotide hydrolysis. To compare the structure of protofilaments in a "GTP-like" conformation with those in a "GDP-like" conformation, we have trapped the GTP state using the nonhydrolyzable analog of GTP, GMPCPP. Previous studies have shown that the properties of GMPCPP microtubules are very similar to those of microtubules polymerized in the presence of GTP (12, 14). Therefore, GMPCPP as well as other nonhydrolyzable analogues can be considered to mimic closely the GTP form of tubulin. Our results show that during depolymerization, protofilaments released from the ends of GMPCPP and GDP microtubules are curved. The degree of curvature seemed to be independent of increasing rates of depolymerization; although a 10-fold increase in calcium concentration increases the rate of depolymerization by about 5-fold, the radius of curvature does not increase (Table 1). Furthermore, the radius of curvature for cold and calcium depolymerization is the same. Taken together, these data suggest both that we are seeing the intrinsic curvature of the protofilaments and that calcium destabilizes microtubules by other mechanisms such as weakening of interprotofilament bonds (19, 26).

Nevertheless, GMPCPP protofilaments have a different curvature from GDP protofilaments. The most likely reason for this result is that the conformation of tubulin subunits liganded with GMPCPP is different from that of subunits liganded with GDP. This idea is consistent with previous results obtained on the structure of GMPCPP and GDP microtubules (14). Tubulin molecules in GMPCPP microtubules were found to be $\approx$0.3 nm longer than in GDP microtubules. In analogy to the proposed existence of a "straight" GTP and a more "curved" GDP conformation (21, 27), this size change was interpreted as a difference in curvature between GMPCPP and GDP subunits, although a change in the bond angle between the tubulin dimers could not be excluded (14). With the recent high resolution structure of tubulin from zinc sheets, it should be possible in the near future to understand the exact structural differences between GMPCPP tubulin and GDP tubulin.

Our data support the model that microtubules are destabilized by an increase in curvature of protofilaments induced by GTP hydrolysis (21). Whereas previous models have proposed a change in protofilament structure from straight to curved (19), we have shown that a GMPCPP, and therefore probably a GTP protofilament, is not straight but has an intrinsic curvature of its own. Thus, during polymerization, the curvature of GTP protofilaments is probably constrained within the microtubule lattice. How could the change in curvature induced by GTP hydrolysis destabilize microtubules? The microtubule wall is stabilized by interactions between protofilaments and destabilized by the tendency of protofilaments to curl away from the lattice (14, 18, 19). The curvature change induced by GTP hydrolysis must be constrained within the microtubule lattice. This constraint would induce mechanical strain on the lateral interactions between protofilaments in the microtubule wall. Thus, our data support the idea in which some of the chemical energy from GTP hydrolysis is stored in the lattice as mechanical strain, ready to be released when depolymerization is triggered (19, 28, 29).

We thank Tim Mitchison and Joe Howard for helpful discussions on the work and T. Ashford, J. Bereiter-Hahn, S. Cohen, S. Eaton, P. Gönczy, M. Glotzer, R. Heald, and S. Reinsch for reading the manuscript. This work was supported by the European Molecular Biology Organization (long-term fellowship to T.M.-R.).

1. Avila, J. (1990) *Microtubule Proteins* (CRC, Boca Raton, FL).
2. Amos, L. & Klug, A. (1974) *J. Cell. Sci.* **14,** 523–549.
3. Mitchison, T. & Kirschner, M. (1984) *Nature (London)* **312,** 237–242.
4. Horio, T. & Hotani, H. (1986) *Nature (London)* **321,** 605–607.
5. Walker, R. A., O'Brien, E. T., Pryer, N. K., Sobeiro, M. F., Voter, W. A., Erickson, H. P. & Salmon, E. D. (1988) *J. Cell Biol.* **107,** 1437–1448.
6. Cassimeris, L., Pryer, N. K. & Salmon, E. D. (1988) *J. Cell Biol.* **107,** 2223–2231.
7. Sammak, P. J. & Borisy, G. G. (1988) *Nature (London)* **332,** 724–726.
8. Carlier, M.-F., Didry, D., Simon, C. & Pantaloni, D. (1989) *Biochemistry* **28,** 1783–1791.
9. Purich, D. L. & Kristoffersen, D. (1984) *Adv. Protein Chem.* **36,** 133–212.
10. Kirschner, M. W. (1978) *Int. Rev. Cytol.* **54,** 1–71.

11. Caplow, M., Ruhlen, R. L. & Shanks, J. (1994) *J. Cell Biol.* **127,** 779–788.
12. Hyman, A. A., Salser, S., Drechsel, D. N., Unwin, N. & Mitchison, T. J. (1992) *Mol. Biol. Cell* **3,** 1155–1167.
13. Audenaert, R., Heremans, L., Heremans, K. & Engelborghs, Y. (1989) *Biochim. Biophys. Acta* **996,** 110–115.
14. Hyman, A. A., Chrétien, D., Arnal, I. & Wade, R. H. (1995) *J. Cell Biol.* **128,** 117–125.
15. Erickson, H. P. (1974) *J. Cell Biol.* **60,** 153–167.
16. Simon, J. R. & Salmon, E. D. (1990) *J. Cell Sci.* **96,** 571–582.
17. Chrétien, D., Fuller, S. D. & Karsenti, E. (1995) *J. Cell Biol.* **129,** 1311–1328.
18. Kirschner, M. W., Williams, R. C., Weingarten, M. & Gerhart, J. C. (1974) *Proc. Natl. Acad. Sci. USA* **71,** 1159–1163.
19. Mandelkow, E. M., Mandelkow, E. & Milligan, R. A. (1991) *J. Cell Biol.* **114,** 977–991.
20. Warner, F. D. & Satir, P. (1973) *J. Cell Sci.* **12,** 313–326.
21. Melki, R., Carlier, M.-F., Pantaloni, D. & Timasheff, S. N. (1989) *Biochemistry* **28,** 9143–9152.
22. Ashford, T., Andersen, S. & Hyman, A. A. (1988) in *Cell Biology, a Laboratory Handbook*, ed. Celis, J. E. (Academic, San Diego), 2nd Ed., Vol. 2, pp. 205–212.
23. Mitchison, T. & Kirschner, M. (1984) *Nature (London)* **312,** 232–237.
24. Porter, M. E. & Johnson, K. A. (1983) *J. Biol. Chem.* **258,** 6575–6581.
25. Field, C. M., Al-Awar, O., Rosenblatt, J., Wong, M. L., Alberts, B. & Mitchison, T. J. (1996) *J. Cell Biol.* **133,** 605–616.
26. Tran, P. T., Joshi, P. & Salmon, E. D. (1997) *J. Struct. Biol.* **118,** 107–118.
27. Howard, W. D. & Timasheff, S. N. (1986) *Biochemistry* **25,** 8292–8300.
28. Mickey, B. & Howard, J. (1995) *J. Cell Biol.* **130,** 909–917.
29. Hyman, A. A. & Karsenti, E. (1996) *Cell* **84,** 401–410.